

## Hybrid Nanocomposites

DOI: 10.1002/ange.200503067

**Emission Enhancement by Formation of Aggregates in Hybrid Chromophoric Surfactant Amphiphile/Silica Nanocomposites\*\****Chetan Jagdish Bhongale and Chain-Shu Hsu\**

Following to the recent development of the organic-templated growth of materials, new types of photonic hybrid composite materials have emerged whose structure and function are organized hierarchically. Ordered, periodic mesoscopic materials allow the construction of composites with many types of guest, such as organic molecules or polymers. These host–guest materials combine the high stability of the inorganic host system, a new structure-forming mechanism due to the confinement of guests in well-defined

---

[\*] C. J. Bhongale, Prof. C.-S. Hsu  
Department of Applied Chemistry  
National Chiao-Tung University  
Hsinchu, Taiwan (R.O.C.)  
Fax: (+ 886) 3513-1523  
E-mail: cshsu@mail.nctu.edu.tw

[\*\*] We thank the National Science Council of the Republic of China (NSC94-2129M009-009) for financial support.



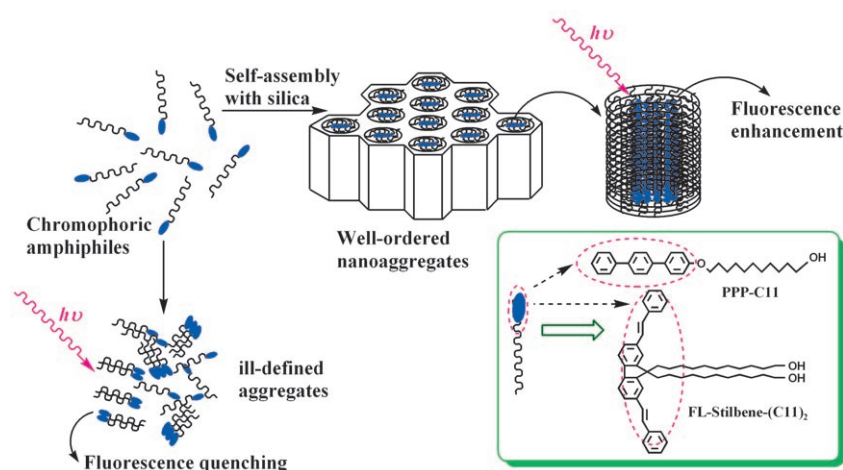
Supporting information for this article is available on the WWW under <http://www.angewandte.org> or from the author.

pore channels, and a modular composition. The inorganic framework serves to protect, stabilize, and orient the organic moiety inside it. Preparation methods, properties, and possible applications of chromophores in porous silica, molecular sieves, and minerals have been summarized in a recent review article.<sup>[1]</sup> Inclusion of dye molecules such as Coumarin 40, Rhodamine BE50, or Oxazine 1 inside the nanopores has been demonstrated by Schulz-Ekloff's and Wöhrle's group,<sup>[2–4]</sup> and in several other papers on this topic the concentration of dye molecules within the mesopores has been optimized by either inclusion of the dye molecules within preformed mesopores or during sol–gel synthesis. These materials showed an increase in photoluminescence intensity at only moderate dye concentrations.<sup>[5–7]</sup> An MEH-PPV/silica nanocomposite<sup>[8]</sup> that was produced for control of energy transfer and prepared by infiltration of MEH-PPV into a preformed, oriented, hexagonal silica mesophase was found to be heterogeneous, exhibiting two distinct conjugated polymer environments, that is, polymers inside and outside the hexagonally arranged pore channels of the silica particles.

Self-assembly is the spontaneous organization of materials (or micelles) through noncovalent interactions without external intervention<sup>[9]</sup> into periodic hexagonal, cubic, or lamellar mesophases. It typically employs nonsymmetric molecules that are programmed to organize into well-defined supramolecular assemblies.<sup>[9]</sup> Amphiphilic surfactant molecules or polymers bearing hydrophilic and hydrophobic parts are the most common examples. Despite the excellent control of pore size, early mesoporous materials, following the pioneering work at Mobil on surfactant-templated materials,<sup>[10]</sup> were isolated in the form of powders, which precludes their use in thin-film applications like membranes, catalysts, etc. Stable, supported, mesoporous silica films were first prepared by the groups of Ozin<sup>[11]</sup> and Brinker<sup>[9,12]</sup> by evaporation-induced self-assembly (EISA). These films can be processed into porous or composite mesostructures with potential utility for a variety of applications such as membranes,<sup>[13]</sup> sensors,<sup>[14]</sup> waveguides,<sup>[15]</sup> lasers,<sup>[4,15,16]</sup> low-dielectric-constant (low- $k$ ) insulators,<sup>[17,18]</sup> and other still-evolving fields of activities. More recently, Okabe et al.<sup>[19]</sup> have demonstrated the immobilization and tuning of one-dimensional, columnar, charge-transfer (CT) assemblies in mesoporous silica films consisting of a hexagonal array of nanoscopic channels. The fabrication and characterization of multiply doped nanostructured silicate sol–gel thin films has also been reported.<sup>[20,21]</sup>

We have exploited the EISA approach to make mesostructured, functional, hybrid nanocomposite films for potential use in electroluminescence devices, where fluorescence quenching in the solid state is the most challenging problem. EISA can organize hydrophilic, inorganic and hydrophobic, organic precursors into ordered nanostructures.<sup>[22]</sup> It is well known that organic nanoparticles have special properties that lie between the properties of molecules and those of bulk materials,<sup>[23]</sup> and aggregation-induced emission (AIE)

enhancement has been observed for a diverse range of conjugated organic nanoparticles.<sup>[24–26]</sup> However, these studies were focused mostly on the photophysical properties of nanoparticle suspensions rather than using nanoparticles systematically in thin-film formation. We have designed and synthesized the amphiphilic surfactant organic compounds PPP-C11 and FL-stilbene-(C11)<sub>2</sub>, which have special conjugated chromophoric groups at the ends of their hydrophobic tails (see Scheme 1 for the chemical structures and the



**Scheme 1.** Formation of the chromophore-bearing amphiphile/silica self-assembled hybrid nanocomposite and the chemical structures of the chromophore amphiphiles used.

Supporting Information for synthetic procedures and characterization data). Our basic idea was to form the core or clusters of the chromophoric groups as nanopackets by self-assembly, which could enhance the photoluminescence (PL) of the nanocomposite films prepared, a seemingly ideal solution for the solid-state quenching of fluorescence. Indeed, we observed a higher photoluminescence intensity and quantum efficiency depending on the orientation and packing of the chromophoric groups at the tail end. The chromophore amphiphiles act as photoactive molecules as well as structure-directing agents. The organic–inorganic functional hybrid nanocomposites were characterized by SEM, TEM, XRD, and steady-state-absorbance and photoluminescence measurements.

The SEM image in Figure 1a shows the formation of nanosheets of the PPP-C11 nanocomposite that are somewhat

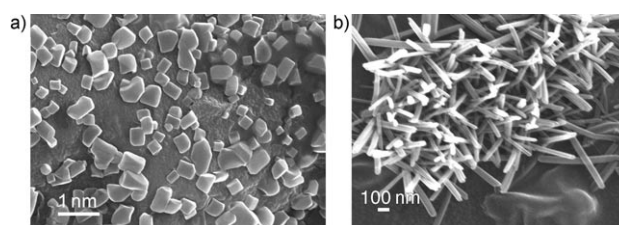


**Figure 1.** SEM images of the chromophoric amphiphile/silica self-assembled nanocomposites formed from a) PPP-C11 and b) FL-Stilbene-(C11)<sub>2</sub>.

rectangular in shape and a few nanometers thick. The FL-stilbene-(C11)<sub>2</sub> nanocomposite formed as uniform nanorods with diameters of about 75 nm and lengths below 1  $\mu\text{m}$  (Figure 1b). X-ray diffraction (XRD) analysis of the nanocomposite thin films showed peaks characteristic of a periodic, mesoscopic silicate structure with single peaks around  $2\theta = 1.53$  and  $1.57^\circ$ , thus indicating periodic, short-range structural order with a  $d$ -spacing for the (100) diffraction peak of 57.9 and 56.2 Å for the nanocomposite films of PPP-C11 and FL-stilbene-(C11)<sub>2</sub>, respectively (Figure 2). The presence of higher-order Bragg peaks

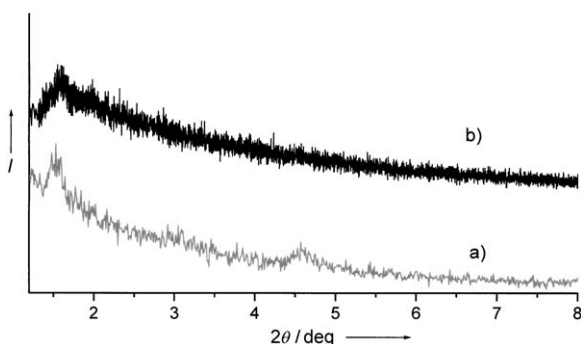


**Figure 2.** XRD profiles of mesostructured chromophoric amphiphile/silica self-assembled nanocomposites formed from a) PPP-C11 and b) FL-Stilbene-(C11)<sub>2</sub>.

around  $2\theta = 3$  and  $4.5^\circ$  in Figure 2a indicates that the PPP-C11 nanocomposite also displays a high degree of long-range structural order. TEM images of the nanocomposites revealed that the composite with FL-stilbene-(C11)<sub>2</sub> has a uniform mesostructure, but with no apparent long-range ordering<sup>[27]</sup> (Figure 3b), whereas the nanocomposite produced with PPP-

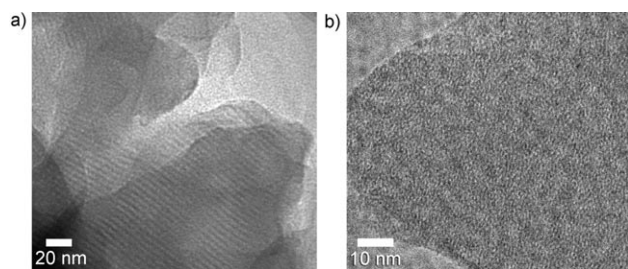


**Figure 3.** TEM images of chromophoric amphiphile/silica self-assembled nanocomposites formed from a) PPP-C11 and b) FL-Stilbene-(C11)<sub>2</sub>.

C11 displays a highly uniform periodic mesostructure (Figure 3a). This difference is due to the size and orientation of the chromophore groups attached at the tail ends and the length and size of the surfactant in the nanocomposites as both these factors affect the topology of amphiphile surfactants and consequently the packing of the chromophores within the channels—the bulkier the group is the greater the steric hindrance, hence the loose packing of the chromophores. Similar results were obtained for the composites prepared by surfactant/silica self-assembly with CTAB and

Brij-58 as surfactant templates.<sup>[27]</sup> We propose that increasing the surfactant tail area, and consequently that of the chromophore, might reduce the value of the surfactant packing parameter ( $g$ )<sup>[28]</sup> and thus affect the mesostructure formation. An apparent decrease in the  $d$ -spacing with respect to the XRD results may be due to the shrinkage of the samples in the TEM chamber.<sup>[29]</sup> Although a future detailed structural study is needed, the present results show that these precursors have the ability to form mesophases by self-assembly.

The UV/Vis absorption and PL spectra for the PPP-C11 nanocomposite are shown in Figure 4a and b, respectively. PPP-C11 is an amphiphile with a terphenyl chromophore as the hydrophobic part and a single alkyl chain with a hydroxy head-group as the hydrophilic part. The absorption band of PPP-C11 in solution in THF is observed at 292 nm, but when a thin film of PPP-C11 is formed its absorption undergoes a blue shift of about 17 nm. The nanocomposite thin film also shows a maximum peak around  $\lambda_{\text{max}} \approx 275$  nm. The PL spectrum of PPP-C11 in THF shows a single band with a maximum peak at 365 nm. In the solid state it undergoes a large decrease, with a maximum peak at 390 nm and two weak shoulders at longer wavelength. This is a red shift of 25 nm relative to the solution spectrum. However, in the nanocomposite we observe a strong emission enhancement in the UV-blue region, with a maximum peak at 390 nm and two pronounced shoulders at 406 and 435 nm with an evident vibrational structure. This fluorescence change, with about a fourteen-fold increase in the intensity, is quite unusual considering that the fluorescence efficiency of organic chromophores generally decreases in the solid state, although they show high fluorescence efficiency in solution. This quite general decrease is attributed mainly to intermolecular vibronic interactions, which induce a nonradiative deactivation process—fluorescence quenching—by excitonic coupling, excimer formation, and excitation energy migration to the impurity traps.<sup>[30]</sup> The emission enhancement observed in the nanocomposite films is due to the well-ordered arrangement of the chromophore groups on the nanoscale. The external quantum efficiency ( $\Phi$ ), as measured by an integrating sphere method, for the PPP-C11 chromophore film is 10%, and this increases to 56% in the PPP-C11 nanocomposite film.

The other chromophore amphiphile studied, FL-stilbene-(C11)<sub>2</sub>, has a bulky chromophore group that contains fluorene and stilbene moieties and two long alkyl chains as the hydrophobic tail, with hydroxy head-groups as the hydrophilic part. A solution of FL-stilbene-(C11)<sub>2</sub> in THF shows an absorption at 372 nm with two shoulders at 355 and 390 nm (Figure 4c). This band is red-shifted for the chromophore and nanocomposite films by 5 nm ( $\lambda_{\text{max}} = 377$  nm) and the shoulder peaks are also shifted to higher wavelengths by about five and ten nanometers, respectively. FL-stilbene-(C11)<sub>2</sub> in THF solution shows bright blue fluorescence with two clearly resolved vibronic features at 410 and 428 nm in the PL spectrum (Figure 4d). In the pure chromophore amphiphile film the PL intensity is quenched and red-shifted, although it still shows the well-resolved vibronic features at 418 and 440 nm and a broad shoulder at longer wavelength.

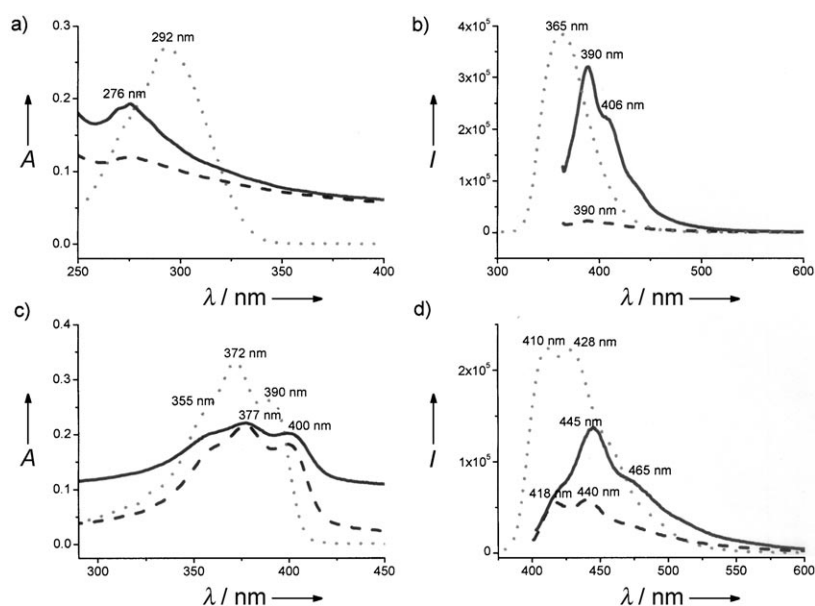


**Figure 4.** UV/Vis spectra for a THF solution (dotted lines) and chromophore (dashed lines) and nanocomposite films (solid lines) of PPP-C11 (a) and FL-Stilbene-(C11)<sub>2</sub> (c). Photoluminescence spectra for a THF solution (dotted lines) and chromophore (dashed lines) and nanocomposite films (solid lines) of PPP-C11 (b) and FL-Stilbene-(C11)<sub>2</sub> (d). (The PL intensities of solutions were normalized for comparison.)

However, when the nanocomposite film of FL-stilbene-(C11)<sub>2</sub> is formed by EISA, its emission intensity is enhanced more than twofold compared to the chromophore amphiphile film alone, with  $\lambda_{\text{max}}$  at 445 nm and shoulders at around 428 and 465 nm. The external quantum efficiency ( $\Phi$ ) for the FL-stilbene-(C11)<sub>2</sub> chromophore film is 24 %, and this increases to 31 % in the FL-stilbene-(C11)<sub>2</sub> nanocomposite film. This increase in absorbance in the nanocomposite indicates an increase in the effective conjugation length of the chromophores and, consequently, enhancement in the fluorescence is observed. The “controlled” aggregation of the chromophore groups within the hydrophobic core of the nanocomposite minimizes the formation of larger crystals and thus enhances the fluorescence. The nanopackets in the hybrid composites could provide a controlled concentration of active dots or chromophores, which are better defined systems, and could prevent coalescence into larger, ill-defined aggregates. A similar enhancement has been observed for C540A residing in the organic, hydrophobic regions of a nanocomposite.<sup>[20]</sup> Although Forster quenching<sup>[31,32]</sup> is observed in most cases for fluorescent molecules in molecular sieves, the fluorescence enhancement induced in this case is attributed to the well-ordered nanopackets of “controlled” chromophore aggregates formed in the self-assembled nanocomposites, as is evident from the above results. The intensity increase may be due to an increased quantum efficiency of the chromophore nanoaggregates within silica. Such a fluorescence enhancement has also been observed for the well-packed chains and aggregates in conjugated polymers<sup>[33]</sup> and for fullerene aggregates in organic–inorganic nanocomposites.<sup>[5]</sup> The mode of interaction amongst the chromophore amphiphile molecules in functional hybrid nanocomposites is a topic

of great research interest and will be discussed in future publications.

In summary, we have demonstrated the preparation of chromophore amphiphile/silica self-assembled nanocomposite films of PPP-C11 and FL-stilbene-(C11)<sub>2</sub> with enhanced emission, and have thus tried to solve the problem of solid-state quenching of organic chromophores. These nanocomposites show a nanosheet or nanorod morphology. The ability to tailor the orientation of the chromophore surfactant amphiphiles within the mesoscopic structures by solvent-evaporation induced self-assembly in thin films, and the subsequent formation of well-ordered chromophore nanopackets, dramatically affects the photophysical properties of these materials. Moreover, this chromophore amphiphile/silica self-assembly approach to overcome the problem of solid-state quenching in the development of organic light emitting devices with high efficiencies should be broadly applicable and will enable new physical studies and new devices with these nanocomposite materials. Furthermore, this method obviates the chromophore leaching problem that is

common in inclusion chemistry. The design of further surfactant amphiphiles with other chromophores at the tail-ends will allow the variation and improvement of the architecture on a molecular and nanometer scale. The demonstration of “controlled” chromophore aggregation and emission enhancement in self-assembled functional hybrid nanocomposites may stimulate new molecular engineering endeavors in the design of luminescent organic compounds with highly emissive aggregation states.

Received: August 29, 2005

Revised: November 18, 2005

Published online: January 30, 2006

**Keywords:** aggregation · fluorescence · nanostructures · organic–inorganic hybrid composites · self-assembly

- [1] G. Schulz-Ekloff, D. Wöhrle, B. van Duffel, R. A. Schoonheydt, *Microporous Mesoporous Mater.* **2002**, *51*, 91.
- [2] M. Ganschow, C. Hellriegel, E. Kneuper, M. Wark, C. Thiel, G. Schulz-Ekloff, C. Bräuchle, D. Wöhrle, *Adv. Funct. Mater.* **2004**, *14*, 269.
- [3] M. Ganschow, M. Wark, D. Wöhrle, G. Schulz-Ekloff, *Angew. Chem.* **2000**, *112*, 167; *Angew. Chem. Int. Ed.* **2000**, *39*, 160.
- [4] M. Ganschow, I. Braun, G. Schulz-Ekloff, D. Wöhrle, *Host–Guest Systems Based on Nanoporous Crystals*, Wiley-VCH, Weinheim, **2003**.
- [5] P. Innocenzi, G. Brusatin, *Chem. Mater.* **2001**, *13*, 3126.
- [6] A. Costela, I. Garcia-Moreno, C. Gomez, O. Garcia, R. Sastre, *Appl. Phys. B* **2002**, *75*, 827.
- [7] C. Peng, H. Zhang, J. Yu, Q. Meng, L. Fu, H. Li, L. Sun, X. Guo, *J. Phys. Chem. B* **2005**, *109*, 15278.



- [8] T.-Q. Nguyen, J. Wu, V. Doan, B. J. Schwartz, S. H. Tolbert, *Science* **2000**, 288, 651.
- [9] C. J. Brinker, Y. Lu, A. Sellinger, H. Fan, *Adv. Mater.* **1999**, 11, 579.
- [10] C. T. Kresge, M. E. Leonowicz, W. J. Roth, J. C. Vartuli, J. S. Beck, *Nature* **1992**, 359, 710.
- [11] H. Yang, N. Coombs, I. Sokolov, G. A. Ozin, *Nature* **1996**, 381, 589.
- [12] Y. Lu, H. Fan, A. Stump, T. L. Ward, T. Rieker, C. J. Brinker, *Nature* **1999**, 398, 223.
- [13] C. Tsai, S. Tam, Y. Lu, C. J. Brinker, *J. Membr. Sci.* **2000**, 169, 255.
- [14] K. Domansky, J. Liu, L.-Q. Wang, M. H. Engelhard, S. Baskaran, *J. Mater. Res.* **2001**, 16, 2810.
- [15] P. D. Yang, G. Wirnsberger, H. C. Huang, S. R. Cordero, M. D. McGehee, B. Scott, T. Deng, G. M. Whitesides, B. F. Chmelka, S. K. Buratto, G. D. Stucky, *Science* **2000**, 287, 465.
- [16] I. Braun, G. Ihlein, F. Laeri, J. Nockel, G. Schulz-Ekloff, F. Schüth, U. Vietze, O. Weiss, D. Wöhrle, *Appl. Phys. B* **2000**, 70, 335.
- [17] R. D. Miller, *Science* **1999**, 286, 421.
- [18] H.-Y. Fan, H. R. Bentley, K. R. Kathan, P. Clem, Y.-F. Lu, C. J. Brinker, *J. Non-Cryst. Solids* **2001**, 285, 79.
- [19] A. Okabe, T. Fukushima, K. Ariga, T. Aida, *Angew. Chem.* **2002**, 114, 3564; *Angew. Chem. Int. Ed.* **2002**, 41, 3414.
- [20] P. N. Minoofar, R. Hernandez, S. Chia, B. Dunn, J. I. Zink, A.-C. Franville, *J. Am. Chem. Soc.* **2002**, 124, 14388.
- [21] P. N. Minoofar, B. Dunn, J. I. Zink, *J. Am. Chem. Soc.* **2005**, 127, 2656.
- [22] A. Sellinger, P. M. Weiss, A. Nguyen, Y. Lu, R. A. Assink, W. Gong, C. J. Brinker, *Nature* **1998**, 394, 256.
- [23] D. Horn, J. Rieger, *Angew. Chem.* **2001**, 113, 4460; *Angew. Chem. Int. Ed.* **2001**, 40, 4330.
- [24] B.-K. An, S.-K. Kwon, S.-D. Jung, S.-Y. Park, *J. Am. Chem. Soc.* **2001**, 123, 14410.
- [25] C. J. Bhongale, C.-W. Chang, C. S. Lee, E. W. G. Diau, C. S. Hsu, *J. Phys. Chem. B* **2005**, 109, 13472–13482.
- [26] J. Luo, Z. Xie, J. W. Y. Lam, L. Cheng, H. Chen, C. Qiu, H. S. Kwok, X. Zhan, Y. Liu, D. Zhu, B. Z. Tang, *Chem. Commun.* **2001**, 1740.
- [27] G. V. Rama Rao, G. P. Lopez, J. Bravo, H. Pham, A. K. Datye, H. Xu, T. L. Ward, *Adv. Mater.* **2002**, 14, 1301.
- [28] Y. Lu, Y. Yang, A. Sellinger, M. Lu, J. Huang, H. Fan, G. Lopez, A. R. Burns, D. Y. Sasaki, J. Shelnutt, C. J. Brinker, *Nature* **2001**, 410, 913.
- [29] B. McCaughey, C. Costello, D. Wang, J. E. Hampsey, Z. Yang, C. Li, C. J. Brinker, Y. Lu, *Adv. Mater.* **2003**, 15, 1266.
- [30] J. B. Birks, *Photophysics of Aromatic Molecules*, Wiley, London, **1970**.
- [31] M. Cotlet, T. Vosch, S. Habuchi, T. Weil, K. Müllen, J. Hofkens, F. De Schryver, *J. Am. Chem. Soc.* **2005**, 127, 9760.
- [32] I. Gopich, A. Szabo, *J. Phys. Chem. B* **2005**, 109, 6845.
- [33] K.-Y. Peng, S.-A. Chen, W.-S. Fann, S.-H. Chen, A.-C. Su, *J. Phys. Chem. B* **2005**, 109, 9368.